

DCOC: an optimality criteria method for large systems

Part I: theory*

M. Zhou and G.I.N. Rozvany

FB. 10, Essen University, D-4300 Essen 1, Germany

Abstract A highly efficient new method for the sizing optimization of large structural systems is introduced in this paper. The proposed technique uses new rigorous optimality criteria derived on the basis of the general methodology of the analytical school of structural optimization. The results represent a breakthrough in structural optimization in so far as the capability of OC and dual methods is increased by several orders of magnitude. This is because the Lagrange multipliers associated with the stress constraints are evaluated explicitly at the element level, and therefore, the size of the dual-type problem is determined only by the number of active displacement constraints which is usually small. The new optimality criteria method, termed DCOC, will be discussed in two parts. Part I gives the derivation of the relevant optimality criteria, the validity and efficiency of which are verified by simple test examples. A detailed description of the computational algorithm for structures subject to multiple displacement and stress constraints as well as several loading conditions is presented in Part II.

1 Introduction

Before explaining the authors' motivation for this new development, the historical background of optimality criteria methods is outlined briefly. The modern history of structural optimization has been marked by the development of two rather independent mainstreams of research, promoted by the so-called *analytical and numerical schools*. The numerical school of structural optimization, dealing with computer-based structural synthesis, was founded over three decades ago by Schmit (1960), who was the first to show the feasibility of coupling finite element analysis and non-linear mathematical programming to create automated optimal design capabilities for a rather broad class of structural systems. During the past three decades, the central task of research activities in this field has been aimed at improving the efficiency of the general strategy used. The necessity for this improvement is due to the facts that

- (A) mathematical programming algorithms need frequent calculations of the objective and constraint functions and their gradients for which very expensive structural and sensitivity analyses are required, and
- (B) the computer time requirement of mathematical programming methods depends largely on the number of design variables which is usually very high for complex engineering structures.

In view of the above, two aspects should be considered for enhancing the efficiency of a specific algorithm:

1. the number of complete structural reanalyses needed for reaching the optimum, and
2. the computer time requirement for the redesign procedure.

Because of the first aspect, the approximation technique introduced by Schmit and his associates (Schmit and Farshi 1974; Schmit and Miura 1976) has become the dominant methodology of structural optimization. In this general approach, the very costly information obtained by structural and sensitivity analyses is used to construct an explicit approximate problem in which the behavioural constraints are typically linearized in terms of either the design variables or their reciprocals, or a mixture of both (Starnes and Haftka 1979). After finding an optimum for the approximate problem, an exact analysis is carried out and a new approximation is constructed. This way the number of exact analyses is reduced considerably.

The second aspect mentioned above concerns the efficiency of the optimization method (i.e. the optimizer) used for solving the approximate problem. As the number of design variables increases, this aspect can become more critical than the first aspect and hence it represents a limiting factor for the capability of a structural optimization algorithm. Discretized optimality criteria methods (DOC) proposed by aerospace scientists (Berke 1970; Venkayya, Khot and Berke 1973), and later in a unified form – known as dual methods – by Fleury (1979), improved this aspect of structural optimization algorithms. In these methods, separable convex approximate problems are transformed into quasi-nonconstrained dual problems in which the variables are Lagrangian multipliers corresponding to the behavioural constraints and hence the only constraints for the dual problem are the nonnegativity requirement of those dual variables. The number of active constraints is often smaller, in some cases much smaller, than the number of design variables. Therefore, the dual problem usually involves fewer variables and only trivial constraints, which gives it a distinct advantage over the primal MP methods for problems where convex separable approximation can be used.

The approximation methodology was generalized in recent years (Vanderplaats and Salajegheh 1988, 1989; Zhou 1989; Zhou and Xia 1990; Canfield 1990) for a much broader class of structures. These authors have realized that for more complex structural systems, such as frames or plates

*Extended version of a paper presented at the 33rd AIAA/ASME/ASCE/AHS/ASC Structures, Structural Dynamics and Materials Conf. in Dallas, April 1992

or some geometrical optimization problems, the behavioural constraints are more directly influenced by some intermediate quantities rather than the design variables themselves. By linearizing the behavioural constraints or some intermediate responses in terms of those intermediate variables, the quality of approximation is highly improved and, therefore, the number of reanalyses is reduced.

Another important general methodology is decomposition (Sobieszcanski-Sobieski *et al.* 1983, 1985), in which a large optimization problem is converted into a set of much smaller, separate but coordinated subproblems. This methodology becomes increasingly important in the rapidly expanding field of multi-disciplinary optimization.

An excellent review of methods of the numerical school is given in a book by Haftka *et al.* (1990).

Concerning the optimization capability of various algorithms, it appeared until recently that the dual method had reached the absolute limit of efficiency. It will be shown in this paper, however, that a further rather dramatic improvement is possible. A new class of optimality criteria methods for cross-sectional optimization problems will be presented on the basis of the general methodology developed by the so-called "analytical school" of structural optimization.

The origin of the analytical approach is usually traced back to the theory of least-weight trusses, developed by Michell (1904) around the turn of the century. This field has been developed very intensively since the sixties by Prager, his associates and others (e.g. Prager and Shield 1967; Prager and Taylor 1968; Masur 1970; Prager and Rozvany 1977; Mróz 1972; Olhoff 1976). A rather broad class of structural optimization problems have been investigated by the analytical school, although closed form solutions were limited to simple, idealized problems. The general methodology used in this field is the so-called continuum-type optimality criteria method (COC), which is based on the Euler-Lagrange type minimality conditions in infinite dimensional design spaces, derived from variational principles. An extensive treatment of the COC method is given by Rozvany (1989) in his recent book.

The fundamental feature of the COC method is that the analysis equations are considered explicitly in the optimization problem as equality constraints. This is a natural feature of *analytical* investigations since no analyser is available for deriving solutions automatically. For the cross-sectional optimization of static systems, the COC formulation has the following characteristics.

- (1) Displacement constraints are formulated by means of the virtual work principle.
- (2) The flexibility formulation for the real and virtual load systems is used and the basic unknowns involved are then the real and virtual forces together with the cross-sectional parameters.
- (3) Kinematical admissibility of the real force system is temporarily omitted in the formulation of the original problem, since the stationarity conditions (i.e. necessary conditions of optimality) imply automatically kinematical admissibility. This also follows from the stationary mutual energy theorem (Shield and Prager 1970; Huang 1971) that states that among all statically admissible solutions, the solution representing stationary mutual energy is also

kinematically admissible.

More recently, an iterative algorithm coupling the COC methods and FE analysis for problems with stress constraints and a single displacement constraint has been developed by the authors (Rozvany and Zhou 1991a, 1991b; Zhou and Rozvany 1991). It has been shown that the COC methods are extremely efficient in handling stress constraints since the latter are uncoupled in the optimality criteria and the corresponding Lagrangians can, therefore, be obtained explicitly at the element level. The effect of active stress constraints is represented by applying modified kinematic conditions for the virtual load system corresponding to the displacement constraint. For example, for beams with constant depth and variable width, the virtual curvature has a given constant value at the cross-section where the flexural stress constraint is active (Rozvany and Zhou 1991a). This modified virtual force system is termed *adjoint system* in the COC methodology. A disadvantage of optimality criteria in the continuum form is that they are not suitable for engineering structures of a discretized nature, and also the adjoint stress-strain relations can be complicated to implement in the FE analysis.

In this paper, discretized optimality criteria methods for structural systems subject to stress constraints and multiple displacement constraints under multiple load conditions are developed on the basis of the fundamental principles of the COC methodology. For historical reasons, we term this approach the DCOC method in order to distinguish it from the DOC methods. General optimality criteria for discretized structural systems are derived on the basis of the flexibility formulation of matrix analysis and Kuhn-Tucker optimality condition. Then, an iterative algorithm for coupling the DCOC method with FE analysis is developed.

For a better understanding of the DCOC algorithm, we can compare it with the very popular semi-intuitive DOC-FSD method, in which the displacement constraints are treated by rigorous optimality criteria but the fully stressed design concept is used for stress constraints. The iterative procedure for the updating phase of the DCOC method is exactly the same as that for the DOC-FSD method. However, rigorous optimality of the DCOC solution is ensured through modifying the virtual load systems for the displacement constraints, by applying initial displacements in members where stress constraints are active.

Table 1 shows the quantities influencing the computer time requirement of the primal MP, dual or DOC, DOC-FSD and DCOC methods in optimizing structural systems with static behavioural constraints where N is the number of design variables, m_d is the number of displacement constraints and m_s is the number of stress constraints. For *large structural systems*, the number of active displacement constraints is usually much smaller than the number of stress constraints, which results in a *very high efficiency of the DCOC method* for such systems. The above contention will also be verified by numerical examples.

With regard to *formulation and derivation of optimality criteria*, the main differences between the DOC and COC/DCOC methods are summarized in Table 2.

In order to demonstrate the fundamental features of the DCOC method, optimality criteria are derived for stress constraints and a *single displacement constraint* in Section 2 and

Table 1. Quantities determining the optimization capability of various methods

| | Primal MP | DOC, Dual | DOC-FSD | DCOC |
|-------------------|-----------|--------------|-------------|---------|
| Critical quantity | N | $m_d + m_s$ | m_d | m_d |
| Solution | Optimal | Optimal | Non-optimal | Optimal |

Table 2. Main differences in the formulation of the DOC and COC/DCOC methods

| | DOC | COC/DCOC |
|---|----------------------------------|--|
| Variables | Design variables | Design variables, Real and virtual forces |
| formulation of stress constraints | through equivalent displacements | directly in terms of real forces |
| equilibrium | implicit | explicit equality constraints |
| compatibility | implicit | not included, implied by optimality |
| calculation of Lagrangians for stress constraints | iteratively, at system level | explicitly, at element level |

the corresponding solution algorithm is presented in Section 3. This algorithm is illustrated with a detailed formulation for trusses in Section 4. Several numerical examples for this class of problems are given in Section 5, where the efficiency of the DCOC method is compared with other methods. Extensions to problems with *multiple displacement constraints* and *multiple loading conditions* are discussed in Section 6, which also includes an illustrative example. The treatment of some difficulties encountered in the DCOC method is discussed in Section 7.

A detailed description of the DCOC computational algorithm for multiple deflection and stress constraints and several load conditions will be given in Part II.

2 Derivation of optimality criteria for linearly elastic structures with stress constraints and one displacement constraint

2.1 Problem formulation

The above class of problems can be stated as

$$\begin{aligned} & \text{minimize } W(\mathbf{x}), \\ & \text{subject to } u_D - u_{Da} \leq 0, \\ & \quad g_j^e(\mathbf{x}) \leq 0 \quad (j = 1, \dots, J_e; e = 1, \dots, N_E), \\ & \quad \mathbf{x} \in \mathbf{x}_F, \end{aligned} \quad (1)$$

where $W(\mathbf{x})$ is the objective function, \mathbf{x} the design variable vector of length N , u_D and u_{Da} , respectively, the displacement at the specified degree of freedom D and the corresponding allowable value, g_j^e with $j = 1, \dots, J_e$ are stress constraints for the e -th element and \mathbf{x}_F is the feasible domain for \mathbf{x} . Denoting the number of elements by N_E , \mathbf{x} can be expressed in N_E partitions

$$\mathbf{x} = \{\mathbf{x}^1 \dots \mathbf{x}^e \dots \mathbf{x}^{N_E}\}^T, \quad (2)$$

in which each partition \mathbf{x}^e of length n_e represents cross-sectional variables of the e -th finite element

$$\mathbf{x}^e = \{x_1^e \dots x_i^e \dots x_{n_e}^e\}^T. \quad (3)$$

The feasible domain \mathbf{x}_F is usually described with lower and upper bounds on the design variables

$$(x_i^e)^L \leq x_i^e \leq (x_i^e)^U \quad (i = 1, \dots, n_e; e = 1, \dots, N_E). \quad (4)$$

The objective function $W(\mathbf{x})$ often represents the weight or volume of the structure.

2.2 Formulation of the behavioural constraints in terms of nodal forces

In order to derive optimality criteria, the relevant behavioural constraints in the original problem (1) will be expressed explicitly in terms of the element nodal forces and the design variables. This can be achieved through the flexibility method of structural analysis (Gallagher 1975; McGuire and Gallagher 1979). The governing equations for a structural system can be expressed as

$$\{\mathbf{P}\} = [\mathbf{B}]\{\mathbf{F}_f\}, \quad (5)$$

$$[\mathbf{B}]^T\{\mathbf{u}\} = [\mathbf{f}]\{\mathbf{F}_f\} + \{\mathbf{u}_{fi}\}, \quad (6)$$

in which $\{\mathbf{P}\}$ is the applied nodal load vector, $[\mathbf{B}]$ the statics matrix, $\{\mathbf{F}_f\}$ a vector of length N_f containing all element nodal forces $\{\mathbf{F}_f^e\}$ according to the flexibility formulation, $\{\mathbf{u}\}$ the nodal displacement vector, $[\mathbf{f}]$ the unassembled global flexibility matrix and $\{\mathbf{u}_{fi}\}$ a vector of length N_f containing all element initial relative displacements $\{\mathbf{u}_{fi}^e\}$ (length n_f). The subscript f of the nodal force and relative displacement vectors refers to degrees of freedom that are free to displace when an element is supported in a stable, statically determinate manner. Relations (5) and (6) are termed, respectively, equilibrium and compatibility equations.

By the principle of virtual work (McGuire and Gallagher 1979), the displacement of the specified degree of freedom D can be expressed as

$$u_D = \sum_{e=1}^{N_E} \{\bar{\mathbf{F}}_f^e\}^T \{\mathbf{u}_f^e\} = \{\bar{\mathbf{F}}_f\}^T [\mathbf{f}]\{\mathbf{F}_f\} + \{\bar{\mathbf{F}}_f\}^T \{\mathbf{u}_{fi}\}, \quad (7)$$

where $\{\bar{\mathbf{F}}_f\}$ are the virtual element nodal forces caused by the virtual unit dummy load $\{\bar{\mathbf{P}}^V\}$ applied at the specified degree of freedom D . If u_D refers to a linear combination of several displacements, then $\{\bar{\mathbf{P}}^V\}$ represent the weighting factors of such a combination. It is important to note that *the real forces $\{\mathbf{F}_f\}$ must satisfy both equilibrium and compatibility conditions and the virtual forces $\{\bar{\mathbf{F}}_f\}$ need only to satisfy the equilibrium conditions*. The equilibrium equations of the virtual load system can be expressed as

$$\{\bar{\mathbf{P}}^V\} = [\mathbf{B}]\{\bar{\mathbf{F}}_f\}. \quad (8)$$

For simplicity, we consider here stress constraints that are linear in terms of the nodal forces. However, generalization to other types of stress constraints is straightforward. The stress constraints g_j^e in (1) can therefore be expressed as

$$g_j^e = \{\mathbf{S}_j^e\}^T \{\mathbf{F}_f^e\} + \{\mathbf{S}_{jd}^e\}^T \{\mathbf{F}_{jd}^e\} - \sigma_{ja}^e, \quad (9)$$

where $\{\mathbf{S}_j^e\}^T$ is a vector converting the element nodal forces into a stress at a specified point j , σ_{ja}^e the permissible stress, $\{\mathbf{F}_{jd}^e\}$ are forces at the point j caused by the distributed load applied within the element e , $\{\mathbf{S}_{jd}^e\}$ is a vector converting $\{\mathbf{F}_{jd}^e\}$ into the stress at the point j . In general, $\{\mathbf{S}_j^e\}$ and $\{\mathbf{S}_{jd}^e\}$ are functions of the element cross-sectional dimensions \mathbf{x}^e , and $\{\mathbf{F}_{jd}^e\}$ contains invariant quantities. Comparing (7) with (9), some fundamental differences between displacement constraints and stress constraints can be noted. Relation (7) implies that the constrained displacement depends on the cross-sectional dimensions and the real and virtual forces of the entire system. On the other hand, a stress constraint concerns only the cross-sectional dimensions and real forces of the relevant element. For this reason, we term displacement constraints *global constraints* and stress constraints *local constraints*. A side constraint is a special kind of local constraints which contains only a single cross-sectional dimension. Relation (9) can also be expressed as

$$g_j^e = \{\mathbf{S}_{jG}^e\}^T \{\mathbf{F}_f\} + \{\mathbf{S}_{jd}^e\}^T \{\mathbf{F}_{jd}^e\} - \sigma_{ja}^e, \quad (10)$$

in which the vector $\{\mathbf{S}_j^e\}$ is extended, by adding zero components, to a vector $\{\mathbf{S}_{jG}^e\}$ which has the same length as $\{\mathbf{F}_f\}$.

Making use of (4), (5), (7), (8) and (10), a relaxed form of the original optimization problem (1) can be expressed as follows:

minimize $W(\mathbf{x})$,

subject to $\{\bar{\mathbf{F}}_f\}^T [\mathbf{f}] \{\mathbf{F}_f\} + \{\bar{\mathbf{F}}_f\}^T \{\mathbf{u}_{fi}\} - u_{Da} \leq 0$,

$$g_j^e = \{\mathbf{S}_{jG}^e\}^T \{\mathbf{F}_f\} + \{\mathbf{S}_{jd}^e\}^T \{\mathbf{F}_{jd}^e\} - \sigma_{ja}^e \leq 0$$

$$(j = 1, \dots, J_e, e = 1, \dots, N_E),$$

$$\{\mathbf{P}\} - [\mathbf{B}]\{\mathbf{F}_f\} = \{\mathbf{0}\},$$

$$\{\bar{\mathbf{P}}^V\} - [\mathbf{B}]\{\bar{\mathbf{F}}_f\} = \{\mathbf{0}\},$$

$$\left. \begin{array}{l} -x_i^e + (x_i^e)^L \leq 0 \\ x_i^e - (x_i^e)^U \leq 0 \end{array} \right\} \begin{array}{l} (i = 1, \dots, n_e; \\ e = 1, \dots, N_E). \end{array} \quad (11)$$

It is important to note that the compatibility conditions (6) for the real force system $\{\mathbf{F}_f\}$ are not involved in (11), and therefore the latter is a relaxed form of (1). However, it will be shown that the stationary solution of this relaxed problem satisfies the compatibility conditions for $\{\mathbf{F}_f\}$ and therefore it also represents the stationary solution of the original problem. The basic variables involved in (11) are the element cross-sectional dimensions \mathbf{x} , the element nodal forces $\{\mathbf{F}_f\}$ of the real system and the element nodal forces $\{\bar{\mathbf{F}}_f\}$ of the virtual system. The entries of $\{\mathbf{u}_{fi}^e\}$ are usually functions of \mathbf{x}^e , but $\{\mathbf{F}_{jd}^e\}$ is independent of \mathbf{x}^e .

2.3 Optimality criteria

The Lagrangian function of the optimization problem in (11) can be written as

$$\mathcal{L} = W(\mathbf{x}) + \nu \left(\{\bar{\mathbf{F}}_f\}^T [\mathbf{f}] \{\mathbf{F}_f\} + \{\bar{\mathbf{F}}_f\}^T \{\mathbf{u}_{fi}\} - u_{Da} \right) +$$

$$\begin{aligned} & + \sum_{e=1}^{N_E} \sum_{j=1}^{J_e} \lambda_j^e \left(\{\mathbf{S}_{jG}^e\}^T \{\mathbf{F}_f\} + \{\mathbf{S}_{jd}^e\}^T \{\mathbf{F}_{jd}^e\} - \sigma_{ja}^e \right) + \\ & + \{\alpha^R\}^T \left(\{\mathbf{P}\} - [\mathbf{B}]\{\mathbf{F}_f\} \right) + \{\alpha^V\}^T \left(\{\bar{\mathbf{P}}^V\} - [\mathbf{B}]\{\bar{\mathbf{F}}_f\} \right) + \\ & + \sum_{e=1}^{N_E} \sum_{i=1}^{n_e} \left[\beta_i^e (-x_i^e + (x_i^e)^L) + \gamma_i^e (x_i^e - (x_i^e)^U) \right], \quad (12) \end{aligned}$$

where ν , λ_j^e , $\{\alpha^R\}$, $\{\alpha^V\}$, β_i^e and γ_i^e are Lagrangian multipliers. The well-known necessary condition for a stationary solution of the problem in (11) is the Kuhn-Tucker condition, which here takes the form

$$\frac{\partial \mathcal{L}}{\partial x_i^e} = 0 \quad (i = 1, \dots, n_e; e = 1, \dots, N_E), \quad (13)$$

$$\frac{\partial \mathcal{L}}{\partial (\mathbf{F}_f)_i} = 0 \quad (i = 1, \dots, N_f), \quad (14)$$

$$\frac{\partial \mathcal{L}}{\partial (\bar{\mathbf{F}}_f)_i} = 0 \quad (i = 1, \dots, N_f). \quad (15)$$

In addition, all Lagrangian multipliers for inequality constraints in (11) must be non-negative. Moreover, if a constraint is not active, then the corresponding multiplier must be zero; $\{\alpha^R\}$ and $\{\alpha^V\}$ are not required to be non-negative because they are Lagrangian multipliers for equality constraints.

Relations (12) and (13) imply

$$\begin{aligned} & \frac{\partial W}{\partial x_i^e} + \nu \left(\{\bar{\mathbf{F}}_f\}^T \left[\frac{\partial \mathbf{f}}{\partial x_i^e} \right] \{\mathbf{F}_f\} + \{\bar{\mathbf{F}}_f\}^T \left\{ \frac{\partial \mathbf{u}_{fi}}{\partial x_i^e} \right\} \right) + \\ & + \sum_{j=1}^{J(e)} \lambda_j^e \left(\left\{ \frac{\partial \mathbf{S}_{jG}^e}{\partial x_i^e} \right\}^T \{\mathbf{F}_f\} + \left\{ \frac{\partial \mathbf{S}_{jd}^e}{\partial x_i^e} \right\}^T \{\mathbf{F}_{jd}^e\} \right) - \beta_i^e + \\ & + \gamma_i^e = 0 \quad (i = 1, \dots, n_e; e = 1, \dots, N_E). \quad (16) \end{aligned}$$

Moreover, by (12), (14) and (15) we have

$$\nu [\mathbf{f}] \{\bar{\mathbf{F}}_f\} + \sum_{e=1}^{N_E} \sum_{j=1}^{J_e} \lambda_j^e \{\mathbf{S}_{jG}^e\} - [\mathbf{B}]^T \{\alpha^R\} = 0, \quad (17)$$

$$\nu ([\mathbf{f}] \{\mathbf{F}_f\} + \{\mathbf{u}_{fi}\}) - [\mathbf{B}]^T \{\alpha^V\} = 0. \quad (18)$$

Here we assume that the displacement constraint is active and therefore $\nu > 0$. Using the notation

$$\{\bar{\mathbf{u}}_{fi}\} = \{\bar{\mathbf{u}}_{fi}^1 \dots \bar{\mathbf{u}}_{fi}^e \dots \bar{\mathbf{u}}_{fi}^{N_E}\}^T, \quad (19)$$

$$\{\bar{\mathbf{u}}_{fi}^e\} = \frac{1}{\nu} \sum_{j=1}^{J_e} \lambda_j^e \{\mathbf{S}_j^e\}, \quad (20)$$

(17) and (18) can be rewritten as

$$[\mathbf{f}] \{\bar{\mathbf{F}}_f\} + \{\bar{\mathbf{u}}_{fi}\} = [\mathbf{B}]^T \{\bar{\mathbf{u}}\}, \quad (21)$$

with

$$\{\bar{\mathbf{u}}\} = \frac{1}{\nu} \{\alpha^R\}, \quad (22)$$

$$[\mathbf{f}] \{\mathbf{F}_f\} + \{\mathbf{u}_{fi}\} = [\mathbf{B}]^T \{\mathbf{u}\}, \quad (23)$$

with

$$\{\mathbf{u}\} = \frac{1}{\nu} \{\alpha^V\}. \quad (24)$$

It can be seen that (23) represents the compatibility conditions for the real force system $\{\mathbf{F}_f\}$ which were omitted in the relaxed problem represented by (11).

Relation (21) provides compatibility conditions for the virtual load system which was not required to be kinematically admissible in the original problem. Since fictitious initial displacements $\{\bar{\mathbf{u}}_{fi}\}$ are involved in the compatibility conditions represented by (21), $\{\bar{\mathbf{u}}\}$ can be interpreted as a fictitious displacement vector. Using the COC terminology (Rozvany 1989), the fictitious system defined by the equilibrium equations (8) and the compatibility equations (21) is termed "adjoint" system. It is important to note that the terminology of "adjoint" has also been used in the field of sensitivity analysis with a different meaning (Haftka *et al.* 1990).

If all stress constraints are inactive, we have $\{\bar{\mathbf{u}}_{fi}\} = \{\mathbf{0}\}$ and (21) reduces to

$$[\mathbf{f}]\{\bar{\mathbf{F}}_f\} = [\mathbf{B}]^T\{\bar{\mathbf{u}}\}, \quad (25)$$

which refers to the standard compatibility equations for the virtual force system. If some of the stress constraints are active, the fictitious initial displacements $\{\bar{\mathbf{u}}_{fi}\}$ given by (19) and (20) are included in the virtual load system. Therefore, the so-called "adjoint" system is, in fact, a *modified virtual load system* in which the structure is subject to both the virtual loads $\{\bar{\mathbf{P}}^V\}$ and fictitious initial displacements $\{\bar{\mathbf{u}}_{fi}^e\}$ ($e = 1, \dots, N_E$).

Since $[\frac{\partial \mathbf{f}}{\partial \mathbf{x}_i^e}]$, $\{\frac{\partial \mathbf{u}_{fi}}{\partial \mathbf{x}_i^e}\}$ and $\{\frac{\partial \mathbf{S}_{jG}^e}{\partial \mathbf{x}_i^e}\}$ in (16) concern, respectively, only the submatrix $[\mathbf{f}^e]$ and subvectors $\{\mathbf{u}_{fi}^e\}$ and $\{\mathbf{S}_j^e\}$ associated with the e -th element, (16) can be rewritten as

$$\begin{aligned} & \frac{\partial W^e}{\partial \mathbf{x}_i^e} + \nu \left(\{\bar{\mathbf{F}}_f^e\}^T \left[\frac{\partial \mathbf{f}^e}{\partial \mathbf{x}_i^e} \right] \{\mathbf{F}_f^e\} + \{\bar{\mathbf{F}}_f^e\}^T \left\{ \frac{\partial \mathbf{u}_{fi}^e}{\partial \mathbf{x}_i^e} \right\} \right) + \\ & + \sum_{j=1}^{J_e} \lambda_j^e \left(\left\{ \frac{\partial \mathbf{S}_j^e}{\partial \mathbf{x}_i^e} \right\}^T \{\mathbf{F}_f^e\} + \left\{ \frac{\partial \mathbf{S}_{jd}^e}{\partial \mathbf{x}_i^e} \right\}^T \{\mathbf{F}_{jd}^e\} \right) - \beta_i^e + \\ & + \gamma_i^e = 0 \quad (i = 1, \dots, n_e; e = 1, \dots, N_E), \end{aligned} \quad (26)$$

where W^e is the contribution of element e to the objective function W .

3 Solution algorithm

3.1 General scheme

In general, all equations governing the optimum design can not be solved simultaneously. For this reason, an iterative algorithm must be employed, and as usual, the following two main steps are involved in each iteration:

- (a) *analysis* of the real and adjoint systems, and
- (b) *updating* of the cross-sectional dimensions \mathbf{x} .

Details of the implementation of the analysis phase will be discussed in the next section.

The governing equations for the updating phase are the optimality criteria in (26) and the active local (stress and side) constraints, as well as the active displacement constraint

$$\varphi = \sum_{e=1}^{N_E} \left(\{\bar{\mathbf{F}}_f^e\}^T \{\mathbf{f}^e\} \{\mathbf{F}_f^e\} + \{\bar{\mathbf{F}}_f^e\}^T \{\mathbf{u}_{fi}^e\} \right) - u_{Da} = 0. \quad (27)$$

The other governing equations will be represented symbolically in the following form.

Optimality criteria [as in (26)]

$$h_i^e(\mathbf{x}^e, \zeta^e, \nu) = 0 \quad (i = 1, \dots, n_e; e = 1, \dots, N_E). \quad (28)$$

Active local (stress and side) constraints

$$\psi_j^e(\mathbf{x}^e) = 0 \quad (j = 1, \dots, m_e; e = 1, \dots, N_E), \quad (29)$$

where ψ_j^e ($j = 1, \dots, m_e$) represent the active stress and side constraints of the e -th element, and $\zeta^e = \{\zeta_1^e, \dots, \zeta_{m_e}^e\}^T$ are the corresponding Lagrangian multipliers.

Once ν is updated on the basis of (27) and (28), then (29) represent N_E uncoupled sets of equations involving only the variables for one element e . Therefore, the natural iterative procedure of the updating phase involves the following two basic steps:

1. update the Lagrangian multiplier ν on the basis of (27);
2. update \mathbf{x}^e and ζ^e ($e = 1, \dots, N_E$) on the basis of N_E uncoupled sets of simultaneous equations (28) and (29).

For the second step of the updating phase ν is considered to have a given value determined in Step 1. If all the local constraints are inactive for the e -th element, then the Lagrangian multipliers corresponding to the local constraints equal zero, and (28) provides n_e equations governing n_e unknowns \mathbf{x}^e . If m_e local constraints (i.e. stress and side constraints) become active, then these equality constraints provide m_e additional equations in the e -th set of equations, and m_e additional unknowns (i.e. the corresponding Lagrangian multipliers) appear in the problem. It follows that (28) and (29) usually determine \mathbf{x}^e and ζ^e sufficiently. However, (28) and (29) become singular if the number of active local constraints is greater than the number of design variables for the e -th set of equations, i.e. $m_e > n_e$. In this case, some equations $\psi_j^e(\mathbf{x}^e) = 0$ [$j = 1, \dots, m_e$] under (29) become dependent, the number of dependent equations being $m_e - n_e$. Therefore, the $n_e + m_e$ unknowns (\mathbf{x}^e, ζ^e) are not given uniquely by the $2n_e < [m_e + n_e]$ independent equations represented by (28) and (29). This situation is experienced in truss optimization when the stress constraint and side constraint of an element are simultaneously active. One way to remove this difficulty is to upgrade $m_e - n_e$ active stress constraints into global constraints. Details of the upgrading technique will be discussed in Section 7.1.

From the above discussion we can see that once the Lagrangian multiplier ν corresponding to the displacement constraint is determined, \mathbf{x}^e and ζ^e can be calculated from (28) and (29) for ($e = 1, \dots, N_E$).

Since $[\mathbf{f}^e]$ and $\{\mathbf{u}_{fi}^e\}$ are functions of design variables \mathbf{x}^e , which depend on ν given by (28) and (29), the displacement constraint in (27) represents an implicit function of ν , i.e.

$$\varphi = \varphi[\mathbf{x}(\nu)]. \quad (30)$$

In general, (28) and (29) are non-separable, nonlinear equations if each element involves several sizing variables. Hence, a rather complicated iterative method must be employed for both steps of the updating operation. However, for a class of simple problems in which only a single design variable x^e is

associated with each element, (28) provides an explicit relation between x^e and ν . This means that an explicit equation can be obtained from (30) for calculating ν and thus the updating algorithm becomes extremely simple. *In order to demonstrate the fundamental features of the proposed method, applications of the DCOC method in this paper are limited to classes of such simple problems.*

Examples of the considered class of problems are as follows:

1. Bernoulli beams with a rectangular cross-section of variable width or variable depth;
2. plane frames with a rectangular cross-section of variable width;
3. trusses of variable cross-sectional areas.

Details of the iterative procedure for trusses is described in Section 4.

3.2 Analysis of the real and adjoint systems

Since the optimization problem and optimality criteria were expressed in terms of forces, the resulting formulation of the real and adjoint systems in (5), (8), (21) and (23) represent standard flexibility formulation. It is well-known that in modern computerized numerical analysis, the flexibility method is much less popular than the stiffness method in which the nodal displacements are the basic unknowns. Thus it is preferable to solve the real and adjoint systems by the stiffness method.

The stiffness equation governing the response of a linear structural system subject to static loading condition is of the form

$$[\mathbf{K}]\{\mathbf{u}\} = \{\mathbf{P}\}, \quad (31)$$

with

$$\{\mathbf{P}\} = \{\mathbf{P}_N\} + \{\mathbf{P}_E\}, \quad (32)$$

where $[\mathbf{K}]$ is the system stiffness matrix, and $\{\mathbf{u}\}$ and $\{\mathbf{P}\}$ are the vectors of unknown displacements and known applied nodal loads. The load vector $\{\mathbf{P}\}$ includes two parts ($\{\mathbf{P}_N\}$ and $\{\mathbf{P}_E\}$), which represent, respectively, the loads applied directly on nodes and the equivalent nodal loads caused by distributed loads applied within the elements, initial displacements and thermal strains. The system stiffness matrix $[\mathbf{K}]$ and load vector $\{\mathbf{P}\}$ can be generated from element level stiffness matrices $[\mathbf{K}^e]$ and equivalent load vector $\{\mathbf{P}_E^e\}$ using an assembly technique known as the direct stiffness method:

$$[\mathbf{K}] = \sum_{e=1}^{N_E} [\mathbf{T}^e]^T [\mathbf{K}^e] [\mathbf{T}^e], \quad (33)$$

$$\{\mathbf{P}\} = \{\mathbf{P}_N\} + \sum_{e=1}^{N_E} [\mathbf{T}^e]^T \{\mathbf{P}_E^e\}, \quad (34)$$

where $[\mathbf{T}^e]$ is the orthogonal transformation matrix of the e -th element. The equivalent nodal loads $\{\mathbf{P}_E^e\}$ are the reversed fixed-end forces $[\mathbf{F}_F^e]$ caused by distributed loads, initial displacements and thermal strains within the e -th element, i.e.

$$\{\mathbf{P}_E^e\} = -\{\mathbf{F}_F^e\}. \quad (35)$$

The element stiffness relationships are

$$\{\mathbf{F}^e\} = [\mathbf{K}^e]\{\mathbf{u}^e\} + \{\mathbf{F}_F^e\}, \quad (36)$$

where $\{\mathbf{F}^e\}$ is the vector of element nodal forces and $\{\mathbf{u}^e\}$ the element nodal displacement vector. Both $\{\mathbf{F}^e\}$ and $\{\mathbf{u}^e\}$ have a length of n_s representing the total number of degrees of freedom of the element. Thus the number of degrees of freedom in the stiffness formulation is by n_r greater than that for the flexibility formulation, where n_r denotes the number of rigid motion, i.e. $n_s = n_f + n_r$. The forces at a point j inside an element include two parts which are the forces caused by the nodal forces $\{\mathbf{F}^e\}$ and the forces caused by the distributed loads applied within the element.

The calculation of fixed-end forces for the real structural system is a standard operation. However, the fixed-end forces for the adjoint system must be generated from the fictitious displacements $\{\bar{\mathbf{u}}_{f_i}^e\}$ given in (19) and (20). We designate $\{\bar{\mathbf{u}}_i^e\}$ of length n_s as the extended adjoint initial displacement vector of $\{\bar{\mathbf{u}}_{f_i}^e\}$, in which the displacements of n_r supported degrees of freedom are set to zero. Then, the fixed-end forces corresponding to the adjoint initial displacements can be expressed as

$$\{\bar{\mathbf{F}}_F^e\} = -[\mathbf{K}^e]\{\bar{\mathbf{u}}_i^e\}, \quad (37)$$

and the equivalent nodal loads are

$$\{\bar{\mathbf{P}}_E^e\} = -\{\bar{\mathbf{F}}_F^e\}. \quad (38)$$

Then, by (34), the load vector for the adjoint system can be expressed as

$$\{\bar{\mathbf{P}}\} = \{\bar{\mathbf{P}}^V\} + \sum_{e=1}^{N_E} [\bar{\mathbf{T}}^e]^T \{\bar{\mathbf{P}}_E^e\}, \quad (39)$$

where $\{\bar{\mathbf{P}}^V\}$ is the virtual load vector corresponding to the displacement constraint.

The solution of the stiffness equation (31) is based on the $[\mathbf{L}][\mathbf{D}][\mathbf{L}]^T$ decomposition and variable bandwidth technique of the stiffness matrix (McGuire and Gallagher 1979). Therefore, the analysis of the adjoint system concerns only once more the forward and backward substitution of the adjoint load vector $\{\bar{\mathbf{P}}\}$.

4 Application to trusses

4.1 Element mechanical relationships

The truss element is shown in Fig. 1. The element force and displacement vectors for the stiffness formulation are

$$\{\mathbf{F}^e\} = \{F_A^e \quad F_B^e\}^T, \quad (40)$$

$$\{\mathbf{u}^e\} = \{u_A^e \quad u_B^e\}^T. \quad (41)$$

The element force-displacement relationships are

$$\{\mathbf{F}^e\} = [\mathbf{K}^e]\{\mathbf{u}^e\}, \quad (42)$$

$$[\mathbf{K}^e] = \frac{E^e A^e}{L^e} \begin{bmatrix} 1 & -1 \\ -1 & 1 \end{bmatrix}, \quad (43)$$

in which A^e is cross-sectional area, E^e Young's modulus and L^e the length of the e -th element. The above element forces, displacements and stiffness matrix are corresponding to the element local coordinate system. The coordinate transformation matrix for a three-dimensional truss can be expressed as

$$[\mathbf{T}^e] = \begin{bmatrix} \cos \alpha & \cos \beta & \cos \gamma & 0 & 0 & 0 \\ 0 & 0 & 0 & \cos \alpha & \cos \beta & \cos \gamma \end{bmatrix}, \quad (44)$$

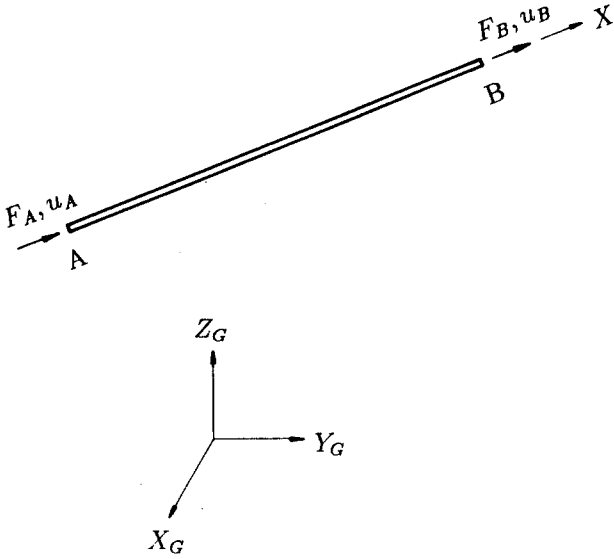


Fig. 1. Truss element

in which α , β and γ are, respectively, the angles between the local element longitudinal axis X and the global system coordinates X_G , Y_G and Z_G .

For a flexibility formulation, the truss element must be supported in a statically determinate manner. Supposing a simple support at end B of the element, the displacement-force relationships are

$$u_{fA}^e = [f_A^e] F_A^e, \quad (45)$$

in which the element flexibility matrix reduces to a single component

$$[f_A^e] = \frac{L^e}{E^e A^e}, \quad (46)$$

and u_{fA}^e in (45) represents the shortening of the e -th element.

4.2 Optimality criteria

The design variables of a truss are the cross-sectional areas of the truss members, i.e. $x^e = A^e$ ($e = 1, \dots, N_E$). The objective function considered is the structural weight which can be expressed as

$$W(\mathbf{x}) = \sum_{e=1}^{N_E} \gamma^e L^e x^e, \quad (47)$$

in which γ^e is the specific weight. Denoting $w^e = \gamma^e L^e$ then (47) can be rewritten as

$$W(\mathbf{x}) = \sum_{e=1}^{N_E} w^e x^e. \quad (48)$$

The optimality criteria will be derived in terms of flexibility relationships. We define the support conditions for an element the same way as for (45). Then, by (7) for the displacement at a specified degree of freedom D we have

$$u_D = \sum_{e=1}^{N_E} \{\bar{\mathbf{F}}_A^e\}^T [f_A^e] \{\mathbf{F}_A^e\} = \sum_{e=1}^{N_E} \frac{\bar{F}_A^e F_A^e L^e}{E^e x^e}. \quad (49)$$

The stress constraints for trusses become

$$g^e = \sigma^e - \sigma_a^e = \frac{|F_A^e|}{x^e} - \sigma_a^e \leq 0 \quad (e = 1, \dots, N_E). \quad (50)$$

By using the optimality criteria in (20) and (26), the stress constraint can be expressed in the standard form shown in (9) as follows:

$$g^e = \{\mathbf{S}^e\}^T F_A^e - \sigma_a^e \leq 0, \quad \text{with } \{\mathbf{S}^e\} = \frac{\text{sgn } F_A^e}{x^e} \quad (e = 1, \dots, N_E). \quad (51)$$

Then by (49) and (51) the optimality conditions given in (26) for the considered problem becomes

$$w^e - \nu \frac{\bar{F}_A^e F_A^e L^e}{E^e (x^e)^2} - \lambda^e \frac{|F_A^e|}{(x^e)^2} - \beta^e = 0 \quad (e = 1, \dots, N_E), \quad (52)$$

where β^e is the Lagrangian multiplier corresponding to the lower side constraint. Upper side constraints are assumed to be inactive in this application.

By (51) the adjoint initial displacements given in (20) can be written as

$$\bar{u}_{fIA}^e = \frac{\lambda^e \text{sgn } F_A^e}{\nu x^e} \quad (e = 1, \dots, N_E), \quad (53)$$

which shows that for the adjoint system initial shortenings exist in those truss elements in which stress constraints are active. By (37) the fixed-end forces of an element corresponding to the adjoint initial displacements can be evaluated from

$$\{\bar{\mathbf{F}}_F\} = -[\mathbf{K}^e] \{\bar{\mathbf{u}}_i^e\}, \quad (54)$$

where $\{\bar{\mathbf{u}}_i^e\}$ is the extended adjoint initial displacement vector

$$\{\bar{\mathbf{u}}_i^e\} = \begin{Bmatrix} \bar{u}_{fIA}^e \\ 0 \end{Bmatrix}. \quad (55)$$

4.3 Iterative algorithm

For the equations governing a truss element, four combinations of active local constraints can be encountered:

R_d : none of the local constraints (stress and lower side constraints) are active;

R_σ : the stress constraint is active;

R_l : the lower side constraint is active, and

$R_{\sigma l}$: both stress and lower side constraints are active.

As already discussed in Section 3.1, the fourth kind of region $R_{\sigma l}$ causes singularity of the equations governing the relevant design variable and Lagrangian multipliers corresponding to the stress and side constraints. In this case, (52) contains two unknowns λ^e and β^e and, therefore, λ^e cannot be evaluated at the element level. A technique for removing this difficulty is to upgrade stress constraints associated with an $R_{\sigma l}$ region into a global constraint which can be expressed in the same way as displacement constraints. Since this technique concerns the problem with multiple displacement constraints, it will be discussed later in Section 7.

It follows that the resizing rule can be expressed as

$$(x^e)^2 = \max\{(x_d^e)^2, (x_\sigma^e)^2, (x_L^e)^2\}, \quad (56)$$

where

$$(x_d^e)^2 = \nu \frac{\bar{F}^e F^e L^e}{E^e w^e}, \quad (57)$$

$$x_\sigma^e = \frac{|F^e|}{\sigma_a^e}, \quad (58)$$

and x_L^e is the lower limit on x^e .

The subscript A of \bar{F}^e and F^e are omitted since the force in a truss member is constant and we have

$$F_A^e = -F^e \quad \text{and} \quad \bar{F}_A^e = -\bar{F}^e \quad (e = 1, \dots, N_E), \quad (59)$$

if we define the sign convention of the forces F^e and \bar{F}^e as positive for tension and negative for compression.

The fixed-end forces corresponding to the adjoint initial displacements can be derived as follows.

For $e \in R_\sigma$, we have $\lambda^e \geq 0$ and then (52) implies

$$\lambda^e = \frac{w^e - \nu \frac{\bar{F}^e F^e L^e}{E^e (x^e)^2}}{\frac{|F^e|}{(x^e)^2}}. \quad (60)$$

Since for $e \in R_\sigma$ (58) applies, (60) can be rewritten as

$$\lambda^e = \frac{1}{\sigma_a^e} \left(w^e x^e - \nu \frac{\bar{F}^e F^e L^e}{E^e x^e} \right). \quad (61)$$

Then, by (43) and (53)-(55) the fixed-end forces corresponding to the adjoint initial displacements can be expressed as

$$\{\bar{\mathbf{F}}\} = \frac{\lambda^e E^e}{\nu L^e} \text{sgn } F^e \begin{Bmatrix} 1 \\ -1 \end{Bmatrix}. \quad (62)$$

The Lagrangian multiplier ν can be derived using the active displacement constraint which by (49) takes the form

$$\sum_{e=1}^{N_E} \frac{\bar{F}^e F^e L^e}{E^e x^e} - u_{Da} = 0. \quad (63)$$

Then by (56)-(58) and (63) we have

$$\nu^{1/2} = \frac{\sum_{e \in R_d} \left(\frac{w^e}{E^e} \bar{F}^e F^e L^e \right)^{1/2}}{u_{Da} - \sum_{e \notin R_d} \frac{\bar{F}^e F^e L^e}{E^e x^e}}. \quad (64)$$

The iterative algorithm for the considered problem is shown in the flow chart given in Fig. 2. The computational steps in Fig. 2 involve the following operations.

- (A) Input of given information defining the problem and of the initial design parameters and performance of one-time computations such as calculating the geometrical parameters of the elements, bandwidth of the stiffness matrix, etc.
- (B) Analysis of the real and adjoint systems. At the first iteration, the adjoint load vector takes simply the virtual loads corresponding to the displacement constraint. For subsequent iterations, the adjoint load vector is the sum of the virtual load vector and the equivalent nodal loads caused by the adjoint initial displacements applied on the elements with active stress constraints (i.e. $e \in R_\sigma$).
- (C) Updating the Lagrangian multiplier ν using (64). The definition of the structural regions R_d , R_σ and R_ℓ comes from the prior iteration. At the first cycle, it is assumed that all elements are displacement controlled, i.e. $e \in R_d$ for $e = 1, \dots, N_E$.
- (D) Updating the cross-sectional parameters \mathbf{x} using (56)-(58).
- (E) The reason for this step is as follows. If the displacement controlled region R_d has changed, then (64) would give an incorrect estimate of ν and hence steps (C) and (D) must be repeated.

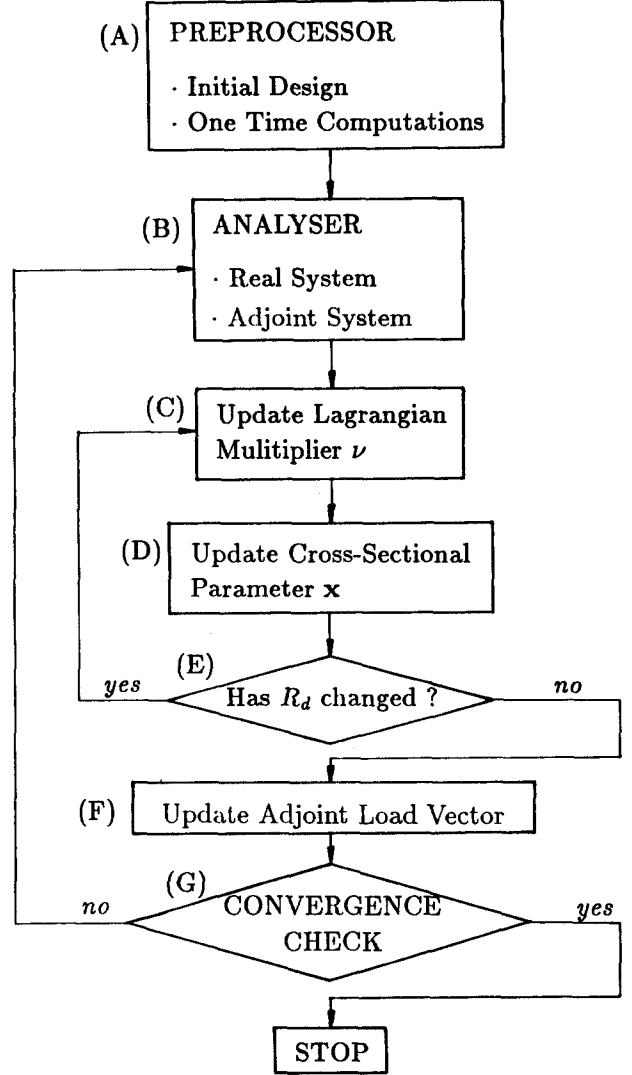


Fig. 2. Flow chart of the DCOC procedure

(F) Updating the adjoint load vector. The equivalent element nodal loads for $e \in R_\sigma$ are the reversed fixed-end forces which can be evaluated from (62).

(G) The convergence criterion is

$$\left| \frac{W_{\text{new}} - W_{\text{old}}}{W_{\text{new}}} \right| \leq T, \quad (65)$$

where T is a given tolerance value.

Since most of the results obtained by DCOC will be compared with those obtained by other methods, a highly accurate solution is desirable. Therefore, unusually stringent tolerance values (e.g. $T = 10^{-8}$) will be employed in the test examples to be presented.

5 Numerical examples

All computational results reported in this paper were obtained on an HP 9000 work station with double precision (FORTRAN 77). For the beams and frames in the second and third examples, details of the formulation of the DCOC method are given elsewhere (Zhou 1992). The dual method used for comparison is based on quadratic approximation of

the objective function and linear approximation of the behavioural constraints in terms of reciprocal variables (Zhou 1989).

5.1 Ten-bar truss

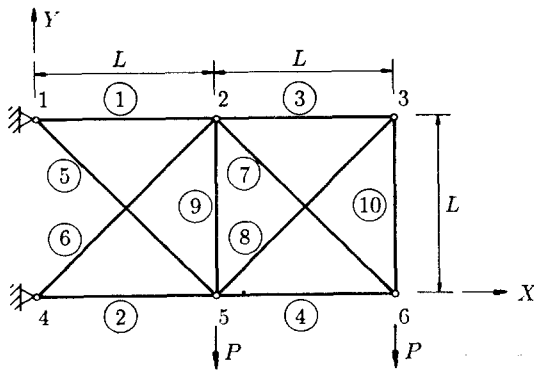
The ten-bar truss shown in Fig. 3 is a well-known example (Haftka *et al.* 1990). A modified version of the ten-bar truss is considered herein, in so far as a displacement constraint is $|v_6| \leq 5.0$ (in), where v_6 is the vertical displacement at node 6. The purpose of this modification is to set a problem, for which the optimal solution contains an R_σ region but no $R_{\sigma\ell}$ region. The material properties are as follows:

$$E^e = 10^7 \text{ psi}, \quad \gamma^e = 0.1 \text{ lb/in}^3, \quad \sigma_a^e = 25000 \text{ psi},$$

$$x_L^e = 0.1 \text{ in}^2 \quad \text{for } (e = 1, \dots, 10).$$

Table 3. Results for the ten-bar truss in Section 5.1

| e | Cross-sectional area (in ²) | | |
|-----------------|---|-----------------|-----------------|
| | DCOC | Dual | DOC-FSD |
| 1 | 12.161173957 | 12.161173956 | 12.126576172 |
| 2 | 8.707029023 | 8.707029026 | 8.827450732 |
| 3 | 0.100000000 | 0.100000000 | 0.100000000 |
| 4 | 6.040579884 | 6.040579884 | 6.046585281 |
| 5 | 5.560164853 | 5.560164853 | 5.564322434 |
| 6 | 8.573640198 | 8.573640196 | 8.497882192 |
| 7 | 8.542669996 | 8.542669996 | 8.551162911 |
| 8 | 0.100000000 | 0.100000000 | 0.100000000 |
| 9 | 0.100000000 | 0.100000000 | 0.100000000 |
| 10 | 0.100000000 | 0.100000000 | 0.100000000 |
| No. of analyses | 24 | 18 | 25 |
| Weight (lb) | 2139.1049799781 | 2139.1049799779 | 2139.1979257067 |



$$L = 360 \text{ in}, P = 10^5 \text{ lb}$$

Fig. 3. Ten-bar truss

Since the purpose of this example is to verify the validity of the DCOC method, a convergence tolerance value of $T = 10^{-12}$ was employed for the DCOC method as well as for the DOC-FSD and dual methods used for comparisons. The results are given in Table 3, which shows that the optimum weight obtained by the DCOC method has 13 significant digits agreement with that of the dual method, and the design variables obtained by these two methods show an at least

9 significant digits agreement. As expected, the DOC-FSD method does not yield the same solution as the other two methods, although it is very close to them.

5.2 Clamped beam with rectangular cross-section of variable width

The beam shown in Fig. 4a has a *variable width*. Since the beam and loads are symmetric, the half beam shown in Fig. 4b can be considered. Normalized parameters are as follows:

$$\gamma = 1, \quad E = 12, \quad d = 1, \quad q = 1, \quad v_{Da} = 1, \quad a = 1,$$

where γ is the specific weight, E Young's modulus, d the constant beam depth, q the uniformly distributed load, v_{Da} the permissible displacement prescribed at midspan and a the half beam span. The flexural and shear stress constraints are represented by $x^e \leq k_1 |M_{\max}^e|$ and $x^e \leq k_2 |F_{Y\max}^e|$, where M_{\max}^e and $F_{Y\max}^e$ are, respectively, the maximum moment and shear force of the e -th element, and $k_1 = 0.23$ and $k_2 = 0.03$ are given constants.

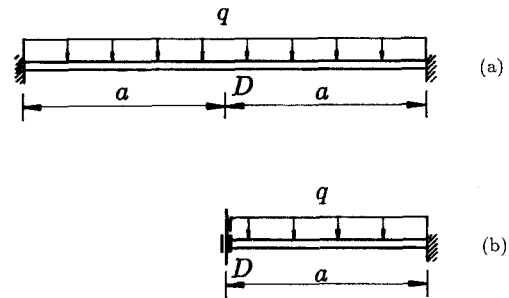


Fig. 4. Clamped beam example

The half beam is discretized into N_E prismatic beam elements. Two models consisting, respectively, of 100 and 1000 elements are considered. For the 100 element model, a convergence tolerance of $T = 10^{-8}$ was used for all computations concerned. The optimum weight and CPU times for the DCOC, DOC-FSD and dual methods are given in Table 4. The CPU times given for "analysis" include those for the analysis of the adjoint system (DCOC), analysis for the virtual load system (DOC-FSD) and sensitivity analysis (dual method). The optimum weight obtained by the DCOC method has an eight significant digits agreement with that of the dual method, and the optimal design variables for these two methods have shown an at least five significant digits agreement (Zhou 1992). Again, the solution of the DOC-FSD method does not show the same degree of agreement with the results of the other two methods. The CPU time needed for the optimization phase of the dual method is much more than that for the DCOC method, since 76 stress constraints and one deflection constraint are active at the optimum. It can be seen that a much larger number of analyses were needed for the DCOC method and DOC-FSD method. This is because in those two methods, the resizing rule for the members with active stress constraint is based on known forces and the dependence of the forces on design variables is not considered. For this reason, the treatment of stress constraints in the resizing procedure of the DCOC and DOC-FSD methods can be regarded as a *zero order approximation*. On the other hand, the dual method is based on *first order*

approximation which achieves a faster convergence. Table 4 shows that about the same analysis time was needed for the dual method with only 9 iterations as for the DCOC method (with 29 iterations). This is because the sensitivity analysis needed by the dual method is very expensive. The optimal width distributions obtained by the DCOC method for both models with 100 and 1000 elements are shown in Fig. 5.

Table 4. Results for the clamped beam example

| 100 Element model | | | | |
|---------------------|--------------|-------------|-------------|-------------|
| | | DCOC | DOC-FSD | Dual |
| Optimal weight | | 0.064202389 | 0.064203018 | 0.064202389 |
| Number of analyses | | 29 | 28 | 9 |
| CPU times (sec.) | optimization | 7.84 | 3.63 | 535.28 |
| | analysis | 116.95 | 112.70 | 117.41 |
| | total | 124.79 | 116.33 | 706.69 |
| 1000 Element model | | | | |
| | | DCOC | DOC-FSD | |
| Optimal weight | | 0.063996543 | 0.063999993 | |
| Number of analyses | | 18 | 20 | |
| CPU times (sec.) | optimization | 57.35 | 34.98 | |
| | analysis | 928.59 | 1126.41 | |
| | total | 985.84 | 1161.39 | |

For the 1000 element model, for which a convergence tolerance of $T = 10^{-6}$ was used, the results of DCOC and DOC-FSD methods are also given in Table 4. The displacement constraint is active in the solutions for both methods. There are 730 active stress constraints in the solution of the DCOC method. Table 4 shows that for both DCOC and DOC-FSD methods the CPU time needed for the optimization phase is a fraction of that needed for the analysis phase. The 1000 element model was not solved by the dual method because, due to over 700 active constraints, the computer time would have been prohibitively high.

5.3 Ten-storey, three-bay frame

The considered frame is shown in Fig. 6, which has 70 elements with rectangular cross-section of variable width. The material properties are as follows:

$$E = 2.1 \cdot 10^7 \text{KN/m}^2, \quad \sigma_a = 3.0 \cdot 10^5 \text{KN/m}^2,$$

$$\tau_a = 5.0 \cdot 10^4 \text{KN/m}^2,$$

where E is Young's modulus, σ_a the permissible flexural stress and τ the permissible shear stress. A horizontal displacement at the left top corner of the frame is constrained to a value of $\Delta \leq 0.3(\text{m})$. The given constant depth is $d = 0.3(\text{m})$ for all the elements. The loading condition is shown in Fig. 6, in which the values of the distributed loads are:

$$q_1 = 10.0 \text{KN/m}, \quad q_2 = 20.0 \text{KN/m}, \quad q_3 = 5.0 \text{KN/m}.$$

With the initial design variables of $x^e = 0.6(\text{m})$ for all elements, a stress constraint violation of 47.6% occurs. A convergence tolerance value of $T = 10^{-4}$ was used. The results of the DCOC method are compared with those of the DOC-FSD and dual methods in Table 5. The reason for small constraint violations in the results of the DCOC and DOC-FSD methods is the *zero order treatment* of stress constraints discussed in Section 5.2. The optimal width distribution is

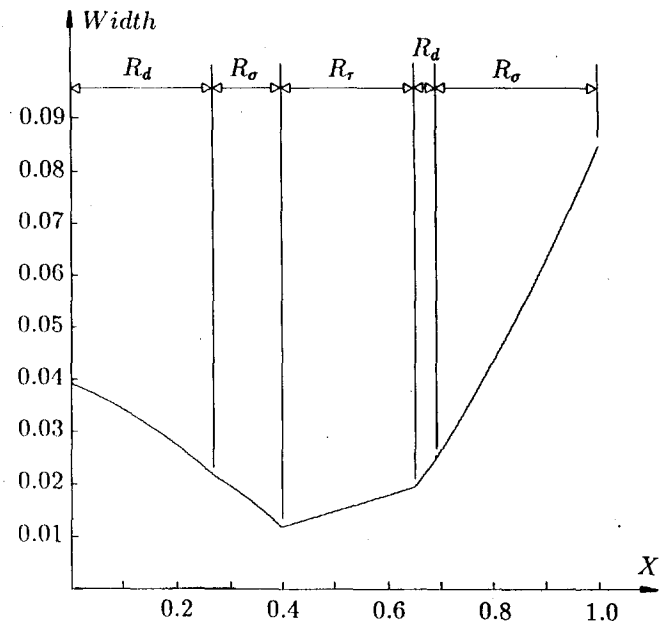
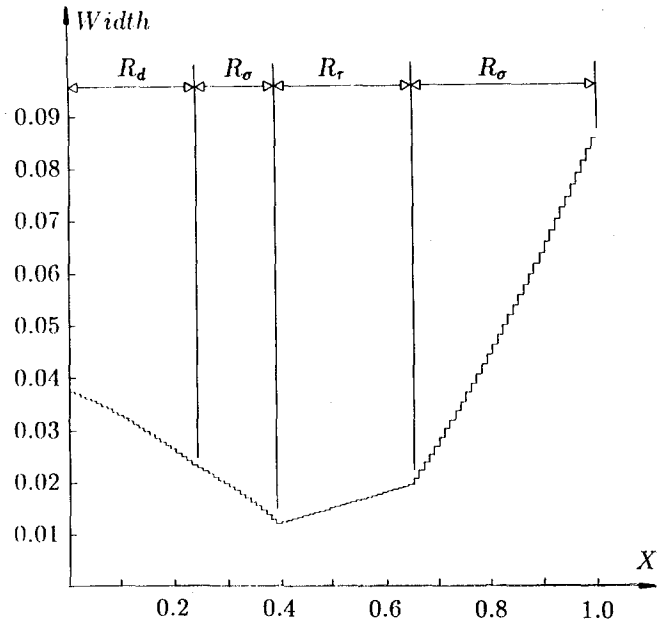


Fig. 5. Optimal width distribution in the beam example: (a) $N_E = 100$, (b) $N_E = 1000$

shown in Fig. 7. For detailed results the reader is referred to Zhou's dissertation (Zhou 1992).

Table 5. Results for ten-storey and three-bay frame

| | | DCOC | DOC-FSD | Dual |
|---------------------------------|--------------|--------|---------|--------|
| Optimal volume (m^3) | | 53.51 | 53.57 | 53.50 |
| Constraint violation | | 0.19 % | 0.74 % | 0.00 % |
| Number of analyses | | 13 | 8 | 12 |
| CPU times (sec.) | optimization | 2.63 | 1.20 | 108.55 |
| | analysis | 49.61 | 34.67 | 197.20 |
| | total | 52.24 | 35.87 | 305.75 |

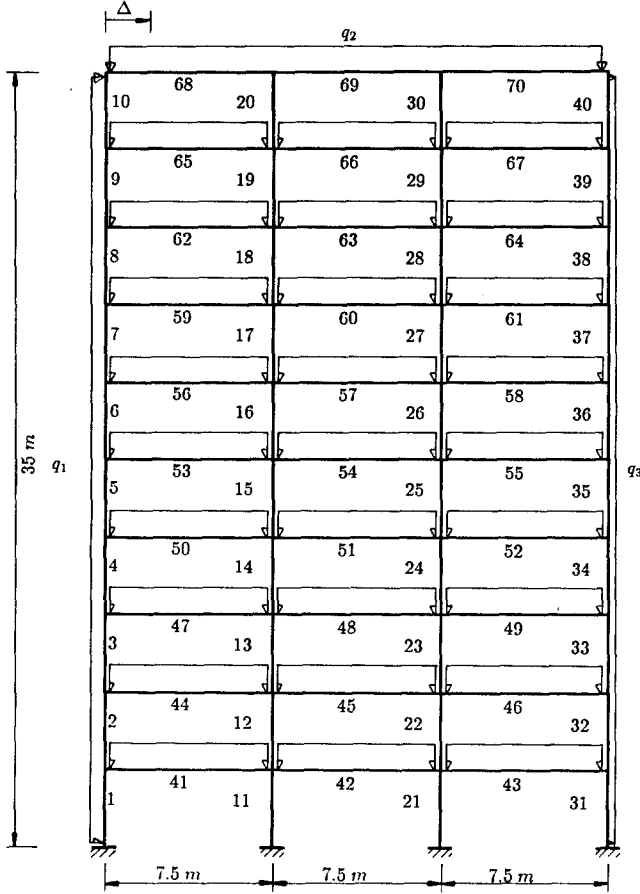


Fig. 6. Multistorey frame example

6 Generalization to multiple displacement constraints and multiple load conditions

6.1 Optimality criteria and solution algorithm

For structural systems subject to multiple displacement constraints together with stress constraints under multiple load conditions, the optimality criteria (26) can be extended as (Zhou 1992)

$$\begin{aligned} & \frac{\partial W^e}{\partial x_i^e} + \sum_{\ell=1}^{N_L} \sum_{k=1}^{N_{D\ell}} \nu_{\ell k} \left(\{\bar{\mathbf{F}}_{f\ell k}^e\}^T \left[\frac{\partial \mathbf{f}^e}{\partial x_i^e} \right] \{\mathbf{F}_{f\ell}^e\} + \right. \\ & \left. + \{\bar{\mathbf{F}}_{f\ell k}^e\}^T \left\{ \frac{\partial \mathbf{u}_{f\ell i}^e}{\partial x_i^e} \right\} \right) + \sum_{\ell=1}^{N_L} \sum_{j=1}^{J_e} \lambda_{j\ell}^e \left(\left\{ \frac{\partial \mathbf{S}_j^e}{\partial x_i^e} \right\}^T \{\mathbf{F}_{f\ell}^e\} + \right. \\ & \left. + \left\{ \frac{\partial \mathbf{S}_{jd}^e}{\partial x_i^e} \right\}^T \{\mathbf{F}_{jld}^e\} \right) - \beta_i^e + \gamma_i^e = 0 \end{aligned} \quad (66)$$

where $\ell = 1, \dots, N_L$ are the load conditions and $k = 1, \dots, N_{D\ell}$ the displacement constraints for the load condition ℓ , $\bar{\mathbf{F}}_{f\ell k}^e$ the adjoint nodal forces associated with the k -th displacement constraint under the ℓ -th loading condition, $\mathbf{F}_{f\ell}^e$ the real nodal forces associated with the ℓ -th load, $\mathbf{u}_{f\ell i}^e$ the initial relative displacements under the ℓ -th load and \mathbf{F}_{jld}^e forces at point j caused by the load acting within the element e under the ℓ -th load. The generalized form of (17) becomes

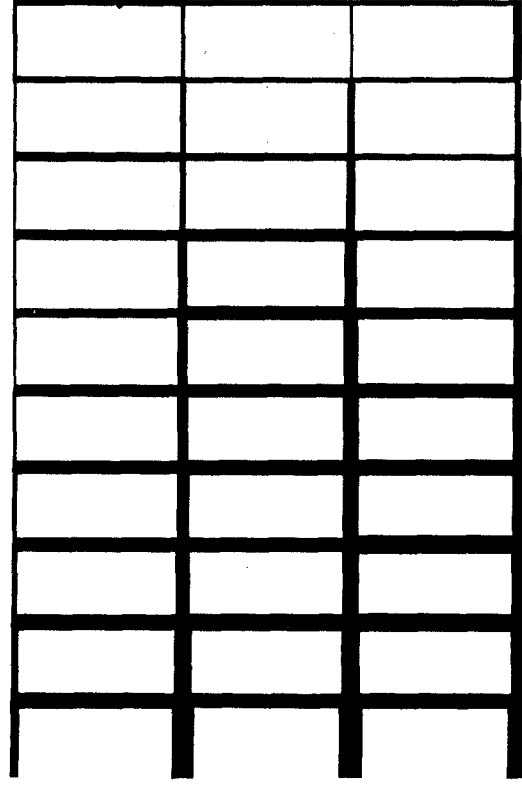


Fig. 7. Optimal width distribution in the frame example

$$\begin{aligned} & \sum_{k=1}^{N_{D\ell}} \nu_{\ell k} \{\mathbf{f}\} \{\bar{\mathbf{F}}_{f\ell k}\} + \{\bar{\mathbf{u}}_{f\ell i}\} = [\mathbf{B}]^T \{\alpha_{\ell}^R\} \\ & (\ell = 1, \dots, N_L), \end{aligned} \quad (67)$$

with

$$\{\bar{\mathbf{u}}_{f\ell i}\} = \sum_{j=1}^{J_e} \lambda_{j\ell}^e \{\mathbf{S}_j^e\}, \quad (68)$$

and (18) is replaced by

$$\begin{aligned} & \nu_{\ell k} \left(\{\mathbf{f}\} \{\mathbf{F}_{f\ell}\} + \{\mathbf{u}_{f\ell i}\} \right) = [\mathbf{B}]^T \{\alpha_{\ell k}^V\} \\ & (\ell = 1, \dots, N_L; k = 1, \dots, N_{D\ell}). \end{aligned} \quad (69)$$

Under the assumption that at least one displacement constraint is active for each load condition, we have by (69)

$$\{\mathbf{f}\} \{\mathbf{F}_{f\ell}\} + \{\mathbf{u}_{f\ell i}\} = [\mathbf{B}]^T \{\mathbf{u}_{\ell}\} \quad (\ell = 1, \dots, N_L), \quad (70)$$

and

$$\{\mathbf{u}_{\ell}\} = \frac{1}{\nu_{\ell k}} \{\alpha_{\ell k}^V\} \quad (\ell = 1, \dots, N_L; k = 1, \dots, N_{D\ell}). \quad (71)$$

Relation (70) implies the compatibility conditions for the real forces $\{\mathbf{F}_{f\ell}\}$ ($\ell = 1, \dots, N_L$). Relation (67) represents N_L sets of compatibility equations governing N_L sets of factorized combination of adjoint forces

$\sum_{k=1}^{N_{D\ell}} \nu_{\ell k} \{\bar{\mathbf{F}}_{f\ell k}\}$, where $\{\bar{\mathbf{F}}_{f\ell k}\}$ ($\ell = 1, \dots, N_L; k = 1, \dots, N_{D\ell}$) are required to be statically admissible, i.e.

$$\begin{aligned} & [\mathbf{B}] \{\bar{\mathbf{F}}_{f\ell k}\} = \{\bar{\mathbf{P}}_{\ell k}^V\}, \\ & (\ell = 1, \dots, N_L; k = 1, \dots, N_{D\ell}). \end{aligned} \quad (72)$$

Relations (67) and (72) represent the compatibility and equilibrium conditions for the virtual load (or “adjoint”) system. If more than one displacement constraint is active for a given load condition ℓ , then a single compatibility condition is not sufficient for determining uniquely the adjoint nodal forces $\bar{\mathbf{F}}_{f\ell k}$. One admissible solution can be obtained by splitting the single compatibility equation for each load case ℓ in (67) into $N_{D\ell}$ compatibility equations. This can be done by introducing the following relations:

$$\{\alpha_{\ell}^R\} = \sum_{k=1}^{N_{D\ell}} \nu_{\ell k} \{\bar{\mathbf{u}}_{\ell k}\} \quad (\ell = 1, \dots, N_L), \quad (73)$$

$$\{\bar{\mathbf{u}}_{f\ell ki}\} = \frac{a_{\ell k}}{\nu_{\ell k}} \{\bar{\mathbf{u}}_{f\ell i}\} \quad (\ell = 1, \dots, N_L; k = 1, \dots, N_{D\ell}), \quad (74)$$

$$\sum_{k=1}^{N_{D\ell}} a_{\ell k} = 1 \quad (\ell = 1, \dots, N_L). \quad (75)$$

Then (67) can be replaced by the following separate compatibility equations:

$$[\mathbf{f}]\{\bar{\mathbf{F}}_{f\ell k}\} + \{\bar{\mathbf{u}}_{f\ell ki}\} = [\mathbf{B}]^T \{\bar{\mathbf{u}}_{\ell k}\} \quad (\ell = 1, \dots, N_L; k = 1, \dots, N_{D\ell}), \quad (76)$$

It is easy to check that (67) is satisfied if (73)-(76) are fulfilled. The property of nonuniqueness of the adjoint forces is still kept since $a_{\ell k}$ ($\ell = 1, \dots, N_L; k = 1, \dots, N_{D\ell}$) can be chosen arbitrarily within the constraint (75).

The general solution algorithm described in Section 3 can also be applied to the multi-displacement and multi-load problems considered in this section. The evaluation of Lagrangian multipliers $\nu_{\ell k}$ ($\ell = 1, \dots, N_L, k = 1, \dots, N_{D\ell}$) becomes the most complex and time consuming task of the updating phase, which can be solved using the equations provided by the active displacement constraints and the relations between the Lagrange multipliers $\nu_{\ell k}$ and design variables \mathbf{x} provided by the optimality criteria (66) and active local constraints. Some techniques (e.g. Newton algorithm) employed in the DOC and dual methods for generating Lagrangian multipliers can be directly used for the DCOC method. The detailed computational algorithm will be presented in Part II of this study. It can be seen easily that, the DCOC method would reduce to the DOC-FSD method if we were to neglect the fictitious initial displacements of the adjoint system in (76). For details of the derivation of the above equations, the reader is referred to Zhou’s doctoral thesis (1992).

6.2 Illustrative example

The ten-bar truss considered in Section 5.1 is used here again as a test example for problems with multiple displacement constraints. The displacement constraints are $|u_6| \leq 1.0$ (in) and $|v_6| \leq 5.0$ (in), where u_6 and v_6 are, respectively, horizontal and vertical displacement of node 6. The other conditions are the same as described in Section 5.1. It has been shown by the dual method that both displacement constraints and the stress constraint at 5-th bar are active at the optimum design. Therefore, it is an ideal example to examine the surprising feature of the adjoint systems outlined in Section 6.1.

The following cases of the DCOC method are tested for the ten-bar truss [see (75)]:

$$\text{Case A : } a_1 = 1, \quad a_2 = 0, \quad (77)$$

$$\text{Case B : } a_1 = 0, \quad a_2 = 1, \quad (78)$$

$$\text{Case C : } a_1 = \frac{\nu_1}{\nu_1 + \nu_2}, \quad a_2 = \frac{\nu_2}{\nu_1 + \nu_2}, \quad (79)$$

where the subscript 1 and 2 refer, respectively, to the displacement constraints on u_6 and v_6 (the first subscript of $a_{\ell k}$ is omitted since we are considering only one loading condition). It is easy to check all the three cases satisfy (76). Although completely different adjoint forces were generated under the above three cases, the final results gave in all three cases “exactly” the same design as the dual method. The results from the DCOC, dual and DOC-FSD methods are indicated in Table 6, for which a convergence tolerance value of $T = 10^{-12}$ was used.

Table 6. Results for the ten-bar truss in Section 6.2

| e | Cross-sectional area (in ²) | | |
|-----------------|---|----------------|----------------|
| | DCOC | Dual | DOC-FSD |
| 1 | 10.8278891 | 10.8278891 | 10.8362276 |
| 2 | 12.2950243 | 12.2950243 | 12.3310330 |
| 3 | 0.1000000 | 0.1000000 | 0.1000000 |
| 4 | 8.6028430 | 8.6028430 | 8.5691720 |
| 5 | 5.6417060 | 5.6417060 | 5.6433667 |
| 6 | 7.6192547 | 7.6192547 | 7.5675629 |
| 7 | 7.6052513 | 7.6052513 | 7.6484854 |
| 8 | 0.1000000 | 0.1000000 | 0.1000000 |
| 9 | 0.1000000 | 0.1000000 | 0.1000000 |
| 10 | 0.1000000 | 0.1000000 | 0.1000000 |
| No. of analyses | A 23 | B 25 | C 23 |
| Weight (lb) | 2220.352475375 | 2220.352475375 | 2220.390773364 |

7 Some difficulties and their treatment

The optimality criteria and iterative algorithm given in Section 6.1 are based on the assumption that at least one displacement constraint is active in each load condition. It is obvious that this assumption is not always satisfied in all design problems. However, in order to restore the validity of the above assumption, one of the stress constraints for the ℓ -th load case can be upgraded into a displacement constraint if no displacement constraint is active for the ℓ -th load case. The same procedure is used for *all* stress constraints in the DOC method. In general, a stress constraint in the form of (9) can be expressed as follows:

$$g_{k\ell}^e = \{\bar{\mathbf{Q}}_k\}^T \{\mathbf{u}_\ell\} - \sigma_{ka}^e, \quad (80)$$

where $\{\bar{\mathbf{Q}}_k\}$ is a vector converting the displacement vector into the relevant stress and σ_{ka}^e is the allowable stress. If we regard $\{\bar{\mathbf{Q}}_k\}$ as a virtual load vector, then the stress constraint $g_{k\ell}^e$ can be considered as a special kind of displacement constraint.

As already discussed in Section 3.1, certain difficulties occur if the number of active local constraints of an element is higher than the number of design variables of this element.

For example, this situation arises in truss design if the stress constraint and lower side constraint are simultaneously active for an element. The above problem can also be solved by upgrading the considered stress constraint into a displacement constraint using the above technique.

7.1 Illustrative example

The technique of upgrading stress constraints into global constraints is illustrated herein by another version of the ten-bar truss considered in Section 5.1. The single displacement constraint is changed to $|v_6| \leq 4.0$ (in) where v_6 represents the vertical displacement of node 6. Other design conditions are exactly the same as those given in Section 5.1. As a result of this modification, the optimal solution contains both R_σ and $R_{\sigma\ell}$ type regions. It was found by using the dual method that the displacement constraint and the stress constraints for the 5-th and 9-th elements are active and the cross-sectional area of the 9-th bar takes the lower side value. Therefore, the DCOC method including the technique of upgrading stress constraints in $R_{\sigma\ell}$ region must be applied.

A convergence tolerance value of $T = 10^{-10}$ is used. The optimum results of the DCOC, DOC-FSD and dual methods are given in Table 7, which shows that the optimum design obtained by the DCOC method is "exactly" the same as that of the dual method. The displacement constraint, stress constraints for the 5-th and 9-th bars and the side constraint of the 9-th bar are active in the solutions of the DCOC and dual methods. The DOC-FSD method gives a significantly different solution in which the side constraint of the 9-th element is not active. A much larger number of analyses is needed by the DOC-FSD method for the considered example.

Table 7. Results for the ten-bar truss in Section 7.1

| e | Cross-sectional area (in ²) | | |
|-----------------|---|---------------|---------------|
| | DCOC | Dual | DOC-FSD |
| 1 | 14.9738773 | 14.9738773 | 15.5500216 |
| 2 | 11.7177294 | 11.7177294 | 11.2224966 |
| 3 | 0.1000000 | 0.1000000 | 0.1000000 |
| 4 | 7.7002256 | 7.7002256 | 7.7176393 |
| 5 | 5.5316570 | 5.5316570 | 5.0834934 |
| 6 | 10.1886802 | 10.1886802 | 10.9668895 |
| 7 | 10.8897635 | 10.8897635 | 10.9143902 |
| 8 | 0.1000000 | 0.1000000 | 0.1000000 |
| 9 | 0.1000000 | 0.1000000 | 0.4168275 |
| 10 | 0.1000000 | 0.1000000 | 0.1000000 |
| No. of analyses | 18 | 16 | 191 |
| Weight (lb) | 2608.76228367 | 2608.76228367 | 2641.76476299 |

Note. The number of iterations used in most test examples of this paper is relatively high due to the unusually stringent convergence criteria used, resulting in an eight to twelve digits agreement between weight values of the DCOC and dual methods. For an accuracy required in practical problems, a much smaller number of iterations is sufficient (see the multi-storey frame example in Section 5.3).

8 Concluding remarks

The following conclusions can be drawn from the results reported in this paper:

- The DCOC method increases the optimization capability by several orders of magnitude for structural systems with a large number of active stress constraints.
- Whilst the iterative procedure for the *updating phase* of the DCOC method is the same as that of the DOC-FSD method, rigorous optimality of the DCOC method is assured through modifying the virtual load systems by applying the appropriate initial displacements in members where the stress constraints are active.
- It is hoped that the DCOC algorithm helps to bridge over the communication gap between the analytical and numerical schools of structural optimization.
- Since topological optimization usually involves an extremely large number of design variables, DCOC is particularly suitable for these problems (Zhou and Rozvany 1991).
- The illustrative examples of this paper were restricted to simple problems involving mainly a single displacement constraint. However, the detailed computational algorithm and several standard test examples for multiple displacement constraints and multiple load conditions will be presented in Part II.

Acknowledgements

The authors are indebted to the Deutsche Forschungsgemeinschaft for financial support (Projekts Ro 744/2-1, Ro 744/4-1, and Ro 744/6-1), to Peter Moche (drafting), Sabine Liebermann (text processing) and Susann Rozvany (editing).

References

- Berke, L. 1970: An efficient approach to the minimum weight design of deflection limited structures. *Rep. Air Force Flight Dynamics Lab. Ohio, USA. AFFDL-TM-70-4*
- Canfield, R.A. 1990: High-quality approximations of eigenvalues in structural optimization. *AIAA J.* **28**, 1116-1222
- Fleury, C. 1979: A unified approach to structural weight minimization. *Comp. Meth. Appl. Mech. Engrg.* **20**, 17-38
- Gallagher, R.H. 1975: *Finite element analysis - fundamentals*. Englewood Cliffs: Prentice-Hall
- Haftka, R.T.; Gürdal, Z.; Kamat, M.P. 1990: *Elements of structural optimization*. Dordrecht: Kluwer
- Huang, N.C. 1971: On principle of stationary mutual complementary energy and its application to structural design. *Zeit. ang. Math. Phys.* **22**, 608-620
- Masur, E.F. 1970: Optimum stiffness and strength of elastic structures. *J. Eng. Mech. Div. ASCE* **96**, 621-640
- McGuire, W.; Gallagher, R.H. 1979: *Matrix structural analysis*. New York: Wiley
- Michell, A.G.M. 1904: The limits of economy of material in frame-structures. *Phil. Mag.* **8**, 589-597
- Mróz, Z. 1972: Multiparameter optimal design of plates and shells. *J. Struct. Mech.* **1**, 371-392

- Olhoff, N. 1976: A survey of optimal design of vibrating structural elements. *Shock and Vibr. Digest*, **8**, 8, 3-10, **8**, 9, 3-10
- Prager, W.; Rozvany, G.I.N. 1977: Optimization of the structural geometry. In: Bednarek, A.R.; Cesari, L. (eds.): *Dynamical Systems*, pp. 265-293. New York: Academic Press
- Prager, W.; Shield, R.T. 1967: A general theory of optimal plastic design. *J. Appl. Mech.* **34**, 184-186
- Prager, W.; Taylor, J.E. 1968: Problems of optimal structural design. *J. Appl. Mech.* **35**, 102-106
- Rozvany, G.I.N. 1989: *Structural design via optimality criteria*. Dordrecht: Kluwer
- Rozvany, G.I.N.; Zhou, M. 1991a: The COC algorithm, part I: cross-section optimization or sizing. *Comp. Meth. Appl. Mech. Engrg.* **89**, 281-308
- Rozvany, G.I.N.; Zhou, M. 1991b: A note on truss design for stress and displacement constraints by optimality criteria methods. *Struct. Optim.* **3**, 45-50
- Schmit, L.A. 1960: Structural design by systematic synthesis. *Proc. 2nd Conf. Electronic Comp.*, pp. 105-122. New York: ASCE
- Schmit, L.A.; Farshi, B. 1974: Some approximation concepts for structural synthesis. *AIAA J.* **12**, 692-699
- Schmit, L.A.; Miura, H. 1976: Approximation concepts for efficient structural synthesis. *NASA CR-2552*
- Shield, R.T.; Prager, W. 1970: Optimum structural design for given deflection. *Zeit. ang. Math. Phys.* **21**, 513-523
- Sobieszcanski-Sobieski, J.; James, B.B.; Dovi, A.R. 1983: Structural optimization by multi-level decomposition. *Proc. AIAA/ASME/ASCE/AHS 24th Structures, Structural Dynamics and Material Conf.* (held in Lake Tahoe, Nevada). AIAA Paper No. 83-0832-CP
- Sobieszcanski-Sobieski, J.; James, B.B.; Riley, F. 1985: Structural optimization by generalized multi-level optimization. *Proc. AIAA/ASME/ASCE/AHS 26th Structures, Structural Dynamics and Material Conf.* (held in Orlando, Fl.). AIAA Paper No. 85-0697-CP
- Starnes, J.H.; Haftka, R.T. 1979: Preliminary design of composite wings for buckling stress and displacement constraints. *J. Aircraft* **6**, 564-470
- Vanderplaats, G.N.; Salajegheh, E. 1988: An efficient approximation technique for frequency constraints in frame optimization. *Int. J. Num. Meth. Engrg.* **26**, 1057-1069
- Vanderplaats, G.N.; Salajegheh, E. 1989: A new approximation method for stress constraints in structural synthesis. *AIAA J.* **27**, 352-358
- Venkayya, V.B.; Khot, S.; Berke, L. 1973: Application of optimality criteria approaches on automated design of large practical structures. *2nd Symp. Struct. Optim.* (held in Milano, Italy), pp. 3.1-3.19, AGARD CP-123
- Zhou, M. 1989: Geometrical optimization of trusses by A two-level approximation concept. *Struct. Optim.* **1**, 235-240
- Zhou, M. 1992: *A new discretized optimality criteria method in structural optimization*. Doctoral Dissertation, Essen University, FB 18/115, Düsseldorf: VDI Verlag
- Zhou, M.; Rozvany, G.I.N. 1991: The COC algorithm, part II: topological, geometrical and generalized shape optimization. *Comp. Meth. Appl. Mech. Engrg.* **89**, 309-336
- Zhou, M., Xia, R.W. 1990: Two-level approximation concept in structural synthesis. *Int. J. Num. Meth. Engrg.* **29**, 1681-1699

Received April 10, 1992

Errata

Struct. Optim. **4**, No. 3-4, Svanberg, K.: "A new approximation of the constraints in truss sizing problems: an explicit second order approximation which is exact for statically determinate truss structures."

p. 170: *First and sixth references*, publisher of the *Proceedings of the NATO ASI "Optimization of large structural systems"* is Kluwer Academic Publishers, Dordrecht

p. 171: *Last equation*, the last term in the denominator should read $x_4x_1x_2$ instead of x_4x_1x .

Third line from the bottom, 75 % should read 0.75 %

Last line, 1.99998 should read 0.99998